Earth and Planetary Science Letters 383 (2013) 113–122

Contents lists available at ScienceDirect

Earth and Planetary Science Letters

www.elsevier.com/locate/epsl

Crustal flow pattern beneath the Tibetan Plateau constrained by regional Lg-wave Q tomography

Lian-Feng Zhao [a,*], Xiao-Bi Xie [b], Jian-Kun He [c], Xiaobo Tian [a], Zhen-Xing Yao [a]

[a] Key Laboratory of the Earth's Deep Interior, Institute of Geology and Geophysics, Chinese Academy of Sciences, Beijing, China
[b] Institute of Geophysics and Planetary Physics, University of California at Santa Cruz, CA, USA
[c] Key Laboratory of Continental Collision and Plateau Uplift, Institute of Tibetan Plateau Research, Chinese Academy of Sciences, Beijing, China

ARTICLE INFO

Article history:
Received 3 May 2013
Received in revised form 19 September 2013
Accepted 19 September 2013
Available online 17 October 2013
Editor: P. Shearer

Keywords:
Lg attenuation
Q tomography
lower-crustal flow
Tibetan Plateau
crustal deformation

ABSTRACT

As a prominent geophysical anomaly, unusually high seismic wave attenuation is observed in the crust and upper mantle of the Tibetan Plateau, particularly along its northern area. Theoretical and laboratory investigations show that the strong seismic attenuation can indicate high temperatures and partial melting, which may decrease the viscosity of the material and cause it to flow. Thus, seismic attenuation distribution may provide useful constraints to the crust flows if they exist. Using Lg-wave Q tomography, we construct a 0.05–10.0 Hz broadband high-resolution crust attenuation model for the Tibetan Plateau and its surrounding regions. The maximum spatial resolution is approximately $1.0^\circ \times 1.0^\circ$ in well-covered areas and for frequencies between 0.05 and 1.5 Hz. This attenuation model reveals an apparent low-Q_{Lg} belt stretching along the northern and eastern Tibetan plateau. Combining the Lg-wave Q model with other geophysical data, two possible crust flow channels are found in the Tibetan Plateau. The main flow channel is from north to east and then turns to southeastern Tibet along the western edge of the rigid Sichuan basin, while a second channel starts from southern Tibet and crosses the Eastern Himalayan syntaxis.

1. Introduction

A lower-crust flow model can explain many geological and geophysical observations in the Tibetan Plateau. Moreover, these observations provide important constraints to the dynamic processes in this region (Klemperer, 2006; Royden et al., 2008; Searle et al., 2011). Typically, the surface strain rates from the Global Positioning System (GPS) and earthquake data are consistent with a gravitationally driven flow model of a viscous lithosphere bounded by strong converging blocks in northern and southern Tibet (e.g., Clark and Royden, 2000; Flesch et al., 2001; Heidbach et al., 2010; Zhang et al., 2004). The low Pn velocities, inefficient Sn propagation, high Poisson's ratios of approximately 0.35, and high seismic Lg-wave attenuation are observed in northern Tibet, suggesting that partial melting is existed within the crust of this region (Fan and Lay, 2003b; Nelson et al., 1996; Owens and Zandt, 1997; Rodgers and Schwartz, 1998). The seismic and magnetotelluric observations revealed that, in eastern and southeastern Tibetan plateau, there are low-velocity and high-conductivity layers in the middle- and lower-crusts, which support a lower-crust flow model (e.g., Bai et al., 2010; Liu et al., 2006; Unsworth et al., 2005; Xu et al., 2007; Yao et al., 2008). However, whether the crust flow is widely spread throughout the entire Tibetan Plateau or is limited to certain narrow geological channels is still under debate. To explore the lower-crust flow pattern throughout the Tibetan Plateau, high-resolution regional measurements of the crust physical properties, such as the velocity, attenuation, anisotropy and electrical structures, are required (e.g., Fan and Lay, 2002; Li et al., 2008; Shapiro et al., 2004; Wang et al., 2013).

Seismic attenuation is usually an indicator of high temperatures and partial melts. An unusually high attenuation in both the crust and upper mantle is one of the first geophysical anomalies discovered in Tibet, particularly in its northern region. The strong Pnl- and Lg-wave attenuations are consistent with the strong Sn-wave attenuation in this region (Fan and Lay, 2003b; Ni and Barazangi, 1983; Rodgers and Schwartz, 1998). Both Rodgers and Schwartz (1998) and Fan and Lay (2003b) suggested that the strong attenuation results from widespread partial melting in the northern Tibetan crust. Xie et al. (2004) found strong crustal Lg-wave attenuation in the Yangbajing graben in southern Tibet and attributed the attenuation to hydrothermal and magmatic fluid activities in the upper-crust. Based on deep seismic sounding data from eastern Tibet, Wang et al. (2007) compared the amplitude difference of seismic PmP waveforms between the observed and synthetic data. They suggested that the weak PmP amplitudes were resulted from a high attenuation in the lower crust and hence suggested

* Corresponding author. Tel.: +86 10 82998658; fax: +86 10 62010846.
E-mail addresses: zhaolf@mail.iggcas.ac.cn (L.-F. Zhao), xxie@ucsc.edu (X.-B. Xie), jkhe@itpcas.ac.cn (J.-K. He).

0012-821X/$ – see front matter © 2013 Published by Elsevier B.V.
http://dx.doi.org/10.1016/j.epsl.2013.09.038

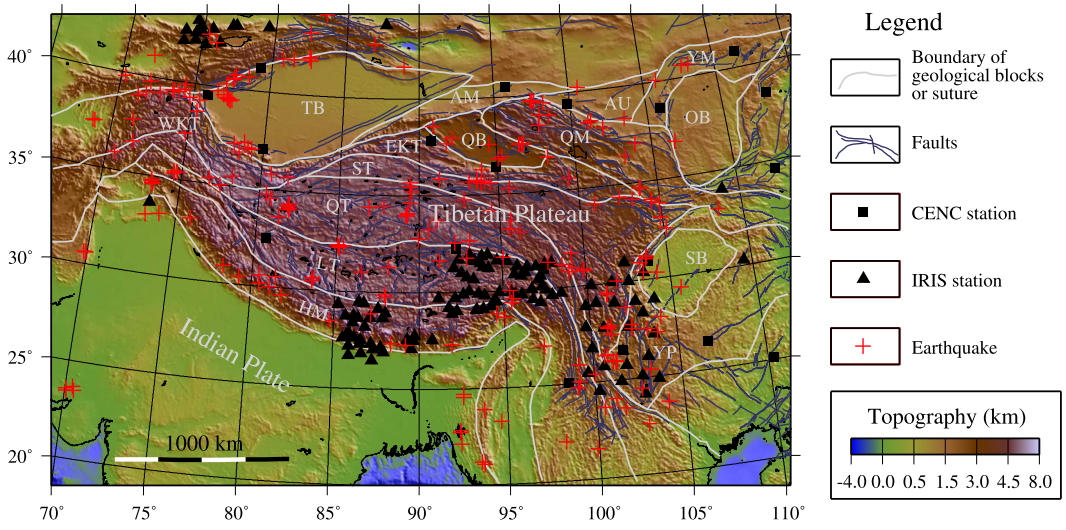

Fig. 1. A topographic map superimposed with main fault systems (light-blue lines), regional tectonics in the Tibetan plateau and its surrounding regions, the locations of the CENC (solid squares) and IRIS (triangles) stations, and the epicenters of selected earthquakes (crosses) used in this study. The information about the major geo-blocks is also listed in Table 1.

that a lower-crust flow was likely existed in this region. In the Tibetan Plateau, previous attenuation studies were mostly limited within local regions or to very low resolutions because of limited data (Bao et al., 2011; Fan and Lay, 2002, 2003a, 2003b; McNamara et al., 1994; Rodgers and Schwartz, 1998; Xie, 2002; Xie et al., 2004; Zhou et al., 2011). Until recently, due to the lack of a high-resolution attenuation model for the Tibetan Plateau, it has been difficult to link the attenuation information with the regional tectonics.

In this study, we develop a high-resolution Lg-wave attenuation model in the Tibetan Plateau and its adjacent regions and investigate its connections to the thermal activities and possible material movement in the lower crust and upper mantle.

2. Data and methods

We collected 7545 broadband vertical-component digital seismograms recorded at 146 stations from 232 regional earthquakes between January 2001 and June 2008 with their ray paths penetrating the plateau. The waveforms were obtained from the China Earthquake Networks Center (CENC) and the Incorporated Research Institutions for Seismology (IRIS) consortium. The station parameters, including code, location, data resource, and affiliation, are listed in Tables S1 and S2 in the supplementary document. Both the CENC and the IRIS stations are equipped with broadband instruments having nearly flat velocity responses from 0.03 Hz to 8.0 Hz and one of the three sampling rates: 20, 40 and 50 points per second. The earthquake parameters are listed in Table S3 in the supplementary document. Shown in Fig. 1 is a topographic map overlapped with the main fault systems (light-blue lines), geotectonics (white lines), locations of the CENC (solid squares) and IRIS (triangles) stations, and epicenters of the earthquakes (crosses) used in this study. The waveforms were selected based on the criteria that these earthquakes were located in the crust, with their magnitudes ranged between $m_b = 3.5$ and 6.0, and the epicenter distances were between 200 and 3000 km. Shown in Figs. S1 and S2 are sample records from an earthquake occurred on June 29, 2002, with S1 filtered between 0.2–2.0 Hz and S2 filtered between 1.0–10.0 Hz. At lower frequencies, the scattering generated P-coda waves are much weaker than at high frequencies.

The data pre-processing was conducted following Zhao et al. (2010, 2013). We extracted the Lg-waveforms using a group-velocity window of 3.6–3.0 km/s and collected the noise time series in an equal-length window as the Lg phase before the first-arriving P wave. Then, we calculated Fourier spectra for both the Lg-wave and the noise, sampled the spectral amplitudes, and corrected for the noise effects. As an example, Fig. 2 illustrates this process for event 2004/08/26 at station MC10. In Fig. 2a, the solid and dashed lines denote the amplitude spectra of Lg and pre-P noise, where the circles and triangles denote the samples at 58 frequencies distributed log evenly between 0.05 and 10.0 Hz. From the signal and noise spectral amplitudes, we calculated the signal-to-noise ratios at individual frequencies (shown in Fig. 2b as solid circles). A threshold of 2.0 is shown as a dashed line and was used for rejecting the low quality data. The noise-corrected Lg-wave spectrum is illustrated in Fig. 2c, where points below the threshold are dropped. After batch processing all regional waveforms, we obtained the source-station amplitudes at individual frequencies between 0.05 and 10.0 Hz. Following Xie et al. (2004) and Zhao et al. (2013), we extracted the interstation (dual-station) data for individual frequencies from the source-station (single-station) data. Both dual- and single-station data were used in the joint inversion for the Lg Q distribution and Lg-wave source functions (for details see Zhao et al., 2013). Using a checkerboard method (e.g., Zhao et al., 2013) with variable grid sizes from $0.8° \times 0.8°$ to $2° \times 2°$, we conducted resolution analyses independently for individual frequencies. At each frequency, we combined ±7% checkerboard shaped perturbations to a constant background Q model, and used it to generate a spectra data set. To simulate the noise in real data, a 5% root mean square random noise was added to the spectra data. We then used this synthetic data set as the input of the inversion system and the inverted result was compared to the checkerboard model to estimate the resolution. Fig. 2d summarizes the number of available rays (for dual-station, single-station, and combined data sets) versus frequency, where the shaded areas illustrate the estimated resolutions for particular frequencies.

3. Tomographic model of Lg attenuation

Based on the above mentioned Lg dataset, we obtained a broadband attenuation model for the Tibetan Plateau and its surrounding regions, where Q_{Lg} is distributed geographically as well as at 58 discrete frequencies between 0.05 and 10.0 Hz.